Trypanosomal Nucleoside Hydrolase. Resonance Raman Spectroscopy of a Transition-State Inhibitor Complex†

Hua Deng,‡ Anita W.-Y. Chan,§ Carey K. Bagdassarian,|| Bernardo Estupiñán,|| Bruce Ganem,§ Robert H. Callender,*,‡ and Vern L. Schramm*,||

Department of Physics, The City College of the City University of New York, New York, New York 10031, Department of Chemistry, Baker Laboratory, Cornell University, Ithaca, New York 14853, and Department of Biochemistry, Albert Einstein College of Medicine, Bronx, New York 10461

Received November 7, 1995; Revised Manuscript Received February 26, 1996⊗

ABSTRACT: The transition state for hydrolysis of the N-ribosidic bond of inosine by nucleoside hydrolase has oxocarbenium character and a protonated leaving group hypoxanthine with an sp^2-hybridized C1′ of the ribosyl [Horenstein, B. A., Parkin, D. W., Estupinan, B., & Schramm, V. L. (1991) *Biochemistry 30*, 10788−10795]. These features are incorporated into *N*-(*p*-nitrophenyl)-D-riboamidrazone, a transition-state analogue which binds with a dissociation constant of 2 nM [Boutellier, M., Horenstein, B. A., Semenyaka, A., Schramm, V. L., & Ganem, B. (1994) *Biochemistry 33*, 3994−4000]. Resonance Raman and ultraviolet−visible absorbance spectroscopy has established that the inhibitor binds as the neutral, zwitterionic species. The enzyme stabilizes a specific resonance state characterized by the quinonoid form of the *p*-nitrophenyl group with evidence for ion pairing at the nitro group. Incorporation of ^{15}N into a specific position of the amidrazone reveals that the *exo*-ribosyl nitrogen bonded to the C1′ position carries the proton while that bonded to the *p*-nitrophenyl carbon is unprotonated. This tautomer carries a distributed positive charge centered at the position analogous to C1′ of the ribosyl group at the transition state. The molecular electrostatic potentials for the substrate inosine, the transition state, and the transition-state inhibitor are compared at the van der Waals surface of the molecules. The tautomer of the inhibitor bound to the enzyme bears a striking electrostatic resemblance to the transition state determined by kinetic isotope effect analysis. The spectral and resonance Raman properties of free and enzyme-bound inhibitor have permitted tautomeric assignment of these species and establish that the enzyme substantially changes the electronic distribution of the bound inhibitor toward that of the enzyme-stabilized transition state.

The inosine−uridine nucleoside hydrolase (IU-nucleoside hydrolase) from the trypanosome *Crithidia fasciculata* catalyzes the hydrolysis of the *N*-glycoside linkage of the commonly occurring purine and pyrimidine nucleosides (Parkin et al., 1991). The nucleoside hydrolases are targets for antiprotozoan agents, since the enzymes are widely distributed in the protozoa but are not present in their mammalian hosts (Miller et al., 1984). Nucleoside hydrolases play a major role in purine salvage in protozoa, which differ from their hosts by requiring exogenous purines (Estupiñán & Schramm, 1994).

Kinetic isotope effect studies of IU-nucleoside hydrolase have established that the transition state is characterized by an elongated C−N glycosidic bond, imparting carbocationic character to the ribose (Chart 1; Horenstein et al., 1991). Negatively charged carboxylates have been implicated in the vicinity of the ribose ring oxygen and are proposed to stabilize this transition state.[1] Oxocarbenium ion stabilization is supported by inhibition studies of nucleoside hydrolase,

Chart 1: Structure of Substrate, Transition State, and the Nitrophenylriboamidrazone Inhibitor of IU-Nucleoside Hydrolase

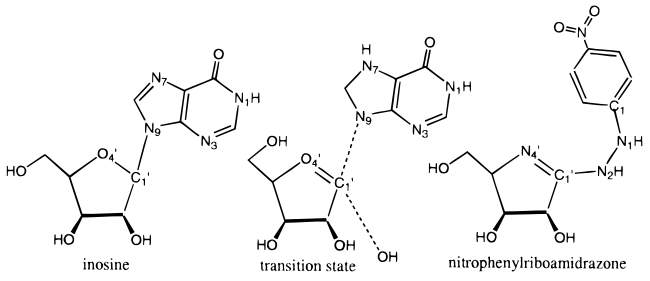

in which inhibitors containing the partial positive ribosyl substitutes bind to the enzyme much tighter than any known substrate (Horenstein & Schramm, 1993a; Boutellier et al., 1994; Chart 1). Greater than −4.9 kcal/mol binding energy is contributed from the interaction between the N4′-H group of the iminoribitol ring and its enzyme environment (Horenstein & Schramm, 1993a,b). *N*-(*p*-Nitrophenyl)-D-ribo-

† This work was supported by Research Grants GM41916 (V.L.S.), GM35712 (B.G.), and GM35183 (R.H.C.) from the National Institutes of Health.

* Address correspondence to these authors.
‡ City College.
§ Cornell University.
|| Albert Einstein College of Medicine.

⊗ Abstract published in *Advance ACS Abstracts,* April 15, 1996.

[1] Recent X-ray crystallographic analysis of the unliganded enzyme and site-directed mutagenesis demonstrate that the presumptive catalytic pocket on IU-nucleoside hydrolase contains four to six carboxylates in a region expected to interact with the ribosyl oxycarbonium at the transition state and a protonated histidine which is proposed to be the proton donor to the hypoxanthine leaving group (Degano et al., 1996; Gopaul et al., 1996).

S0006-2960(95)02654-7 CCC: $12.00

amidrazone (nitrophenylriboamidrazone) binds 2×10^5 more tightly than inosine to IU-nucleoside hydrolase, to yield a dissociation constant of 2 nM (Boutellier et al., 1994). The affinity of a similar inhibitor without the NO_2 group, phenylriboamidrazone, is decreased by 2 orders of magnitude. Addition of the NO_2 group therefore contributes an additional −2.8 kcal/mol to inhibitor binding. Since protonation of the departing hypoxanthine ring at N7 is believed to be a significant feature of the transition state for nucleoside hydrolase (Horenstein & Schramm, 1993a,b), it has been suggested that the NO_2 group of nitrophenylriboamidrazone may be interacting with the enzymic proton donor, proposed to be a protonated histidine.[1]

Raman spectroscopy is well suited to the characterization of enzyme−inhibitor interactions [for review see Callender and Deng (1994)]. The protonation states of a variety of substrate groups, including C═N bonds, can be established when bound to proteins (Deng et al., 1989, 1993a; Goldberg et al., 1993). Studies with nitro compounds have demonstrated that the NO_2 group shows strong Raman bands. These bands would undergo predictable resonance Raman changes if the NO_2 group of bound inhibitor is protonated or strongly hydrogen-bonded. The use of a specifically ^{15}N-substituted inhibitor permits unambiguous assignment of the associated Raman bands. Such studies should reveal the tautomeric state of nitrophenylriboamidrazone in solution and the changes which occur when nitrophenylriboamidrazone is bound to the enzyme. Since nitrophenylriboamidrazone has been proposed to act as a transition-state inhibitor, these studies are expected to reveal features of the catalytic machinery of IU-nucleoside hydrolase.

MATERIALS AND METHODS

IU-Nucleoside Hydrolase and Nitrophenylriboamidrazones. The enzyme was purified to near homogeneity from *C. fasciculata* using the methods published previously (Parkin et al., 1991). Protein purity was confirmed by SDS−polyacrylamide gel electrophoresis to be >95%. *N*-(*p*-Nitrophenyl)-D-riboamidrazone (nitrophenylriboamidrazone) was prepared as described previously (Boutellier et al., 1994). Inhibitor specifically labeled with ^{15}N at the 2-position of the hydrazine (Chart 1) was synthesized from *p*-nitrophenylhydrazine (2-^{15}N). Labeled phenylhydrazine was synthesized by an adaption of a published procedure (Beilstein, 1932). A solution of sodium nitrite (^{15}N) (216 mg, 3.13 mmol) in H_2O (1 mL) was added by separatory funnel to a suspension of *p*-nitroaniline (211 mg, 1.53 mmol) in 37% HCl (1 mL) while being cooled in an ice bath. The reaction mixture was stirred 5 min, and the resulting solution of diazonium salt was neutralized with saturated aqueous $NaHCO_3$ (2 mL). A reducing solution of sodium sulfite was prepared by bubbling SO_2 into aqueous NaOH (367 mg in 2.5 mL of H_2O) for about 5 min and then neutralizing with potassium carbonate (433 mg, 3.14 mmol). The diazonium salt was poured rapidly into the freshly made sodium sulfite solution to give a yellow solid which was filtered, washed with H_2O (2 mL), and redissolved in 6 N HCl (3 mL). The resulting HCl salt was cooled in an ice bath and neutralized with $NaHCO_3$ (0.5 g) and NaOAc (0.5 g). The dark aqueous phase was extracted with diethyl ether (5×50 mL), and the combined organic layers were dried over Na_2SO_4, filtered, and concentrated in vacuo to afford the product as a red solid (45 mg, 20%).

Conversion of *p*-nitrophenylhydrazine (2-^{15}N) to the corresponding *N*-(*p*-nitrophenyl)-D-riboamidrazone was accomplished using the method reported earlier (Boutellier et al., 1994). The ^1H-NMR of the ^{15}N-labeled product matched data reported for the unlabeled amidrazone.

The resonance Raman spectra of nitrophenylriboamidrazone in solution and of the nitrophenylriboamidrazone/nucleoside hydrolase mixture were measured with the 457.8 nm line from an argon ion laser at a power level of 20 mW at the sample. Both enzyme activity and visible absorption spectral features of the inhibitor were measured before and after the Raman experiment. No changes were detected. A small spectral contribution from the enzyme and buffer in the original nitrophenylriboamidrazone/enzyme Raman spectra was subtracted. All experiments were conducted at 4 °C.

The Raman spectra were taken with an optical multichannel analyzer (OMA) system consisting of a triplemate spectrometer (Spex Industries, Metuchen, NJ), a model DIDA-1000 reticon detector connected to a ST-100 detector controller (Princeton Instruments, Trenton, NJ), which was interfaced to a MAC II computer (Apple Computer, Cupertino, CA). With the above laser excitation wavelength, a spectral window of about 1000 cm^{-1} with resolution of 8 cm^{-1} was obtained. The Raman band positions were calibrated against the known Raman peaks of toluene and are accurate to ± 3 cm^{-1}.

pK_a and Spectral Characteristics of Nitrophenylriboamidrazone. Solutions of nitrophenylriboamidrazone (40−100 μM) were prepared from the solid and gave a pH of 5.6 when dissolved in water. Titrations with 0.01 and 0.1 M NaOH and HCl were used to attain pH values between 4.5 and 8.0. The ultraviolet−visible spectrum was measured on a Cary 210 recording spectrophotometer at room temperature. The inhibitor is unstable at pH values above 9.0 or below 4.5, resulting in loss of the isosbestic points near 285 and 367 (Figure 1).

Spectrum of Bound Nitrophenylriboamidrazone. A dual-sector quartz cuvette contained 15 μM nitrophenylriboamidrazone, pH 7.3, in 25 mM Hepes buffer in one sector and 19 μM IU-nucleosidase in the same buffer in the second sector. The visible spectrum was recorded at room temperature. The spectrum was recorded a second time after the solutions in both sectors were mixed.

Molecular Electrostatic Potential Surfaces. Molecular electrostatic potential surface calculations were patterned after methods described previously (Horenstein & Schramm, 1993a,b). Calculations with nitrophenylriboamidrazone (cf. Chart 1 and Figure 5) used dihedral angles of N4′−C1′−N2−N1 and C1′−N2−N1−C1 which were fixed at 0° and 90°, respectively. These angles provide a near-isosteric alignment of the phenyl group with the hydrophobic center of the hypoxanthine ring at the transition state when the dihedral angle formed by C2′−C1′−N9−C8 = 0°. Alignment of the nitro group is near O6 of inosine at the transition state (Boutellier et al., 1994). Electrostatic potential calculations were performed on the neutral form of nitrophenylriboamidrazone to give a distributed charge of +1 across C1′ and −1 at the nitro group. The net charge of the transition state of inosine is also near +1 across the partial positive charge of the oxycarbonium centered primarily at C1′ but also across O4′. The imidazole ring of hypoxanthine and adjacent atoms carry a net negative charge, prior to

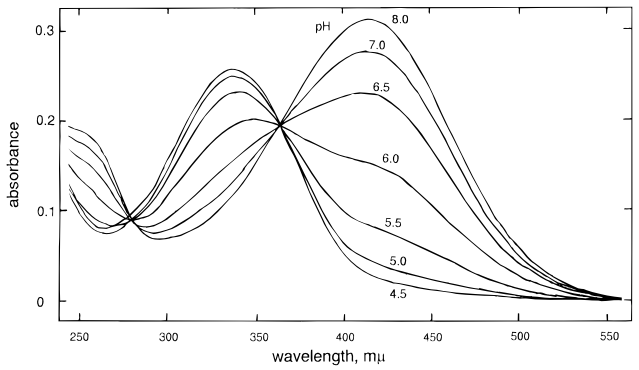

FIGURE 1: Absorbance spectrum of nitrophenylriboamidrazone as a function of pH. Solid nitrophenylriboamidrazone was dissolved in H_2O to give a 65 μM solution, pH 5.6, and the spectrum was recorded (not shown). The solution was adjusted to pH 5.0 with HCl, and the UV−visible spectrum was recorded. The procedure was repeated at pH values of 5.5, 6.0, 6.5, 7.0, and 8.0 to give the spectra of the figure. The same sample was then adjusted again to pH values of 6.0, 4.5, and 6.5 to establish that the spectral properties were stable during the titration. Following the treatments between pH 5.0 and 8.0, the isosbestic points were constant. At pH 4.5, the spectral properties between 310 and 550 nm were unchanged, but spectral features below 310 nm were changed significantly, altering the isosbestic point. At pH values of 9.0 and above, the isosbestic points were also lost.

protonation by the enzyme. Gaussian 92 calculations were used to establish the electronic wave functions for the molecules. Molecular bond angles were constrained to those determined by a combination of experimental kinetic isotope effects and bond-energy bond-order vibrational analysis (Horenstein & Schramm, 1993a,b). Bond lengths were optimized to their energetic minima by iterative analysis prior to calculation of the wave function on the structurally optimized molecules constrained to the configuration of the transition state. Calculations at the STO-3G basis set were found to be adequate to describe the electrostatic potential surface features, when compared to results obtained with the 6-31G basis set.

The wave functions were used to generate maps of the electron density near the van der Waals surface, defined as the level of 0.002 electron per bohr^3 (Venanzi et al., 1992; Sjoberg & Politzer, 1990; Lamotte-Brasseur et al., 1990). The values of the electrostatic potential generated from the CUBE function of Gaussian 92 were interpreted into color maps using AVS and ChemViewer routines (Advanced Visual Systems, Inc., and Molecular Simulations, Inc.). Color assignment was blue for regions with electrostatic potential greater than the average at the surface and red for regions with electrostatic potential lower than average. Thus, blue and red represent partial negative and positive sites, respectively.

RESULTS

Spectral Properties of Nitrophenylriboamidrazone. Titration of nitrophenylriboamidrazone in the pH range of 4.5−8 gave a pK_a value of 6.1 (Figure 1). The λ_{max} of unprotonated nitrophenylriboamidrazone is 420 nm and shifts to 340 nm upon protonation. Within the pH range of 5.0−8.0, the protonation−deprotonation process is fully reversible as indicated by the isosbestic points at 368 and 282 nm. The millimolar extinction coefficients for neutral and protonated inhibitor are 4.8 and 4.0 at 420 and 340 nm, respectively.

Chart 2: Tautomers of Nitrophenylriboamidrazone

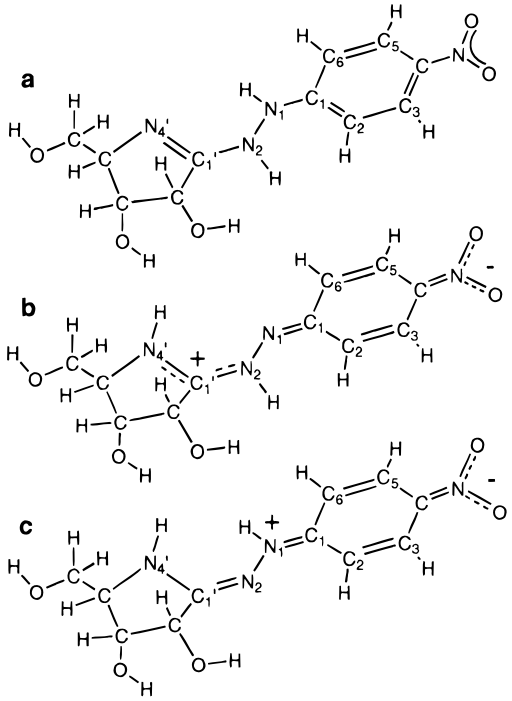

Electrospray mass spectroscopy and gel electrophoresis (data not shown) established that nitrophenylriboamidrazone is neutral at pH 8.0 and is positively charged at pH 4.5. In the neutral form of nitrophenylriboamidrazone at pH 8, two of the three nitrogens of the riboamidrazone moiety are protonated. Three of the numerous tautomers possible at this pH are shown in Chart 2. In tautomer a, N1 and N2 are protonated. This tautomer is unlikely in aqueous solution at pH 8 since the conjugation in this tautomer starting from the NO_2 group is not expected to be extended beyond the phenyl ring and is unlikely to exhibit the strong absorbance at 420 nm which is associated with a nitroquinonoid (Figure 1). Protonation of N4′ of this tautomer at acid pH values would not be expected to cause the observed shift in the absorbance maximum to 340 nm (Figure 1).

Binding to nucleoside hydrolase causes a red shift in the absorption band of nitrophenylriboamidrazone from 420 to 445 nm and increases the molar extinction coefficient. The full width at half-maximum of the absorption band is reduced from 124 nm in solution to 99 nm on the enzyme (Figure 2). These changes suggest that neutral nitrophenylriboamidrazone exists as a mixture of tautomers in solution (Chart 2), whereas on the enzyme, a single tautomer of nitrophenylriboamidrazone may predominate. This notion is reinforced by the resonance Raman data below. The λ_{max} of this tautomer may also be red shifted due to its interaction with the enzyme.

Resonance Raman Spectra of Free Nitrophenylriboamidrazone. The Raman spectra of nitrophenylriboamidrazone in solution at pH 8 and isotopically labeled derivatives are shown in Figure 3. Resonance Raman shows only those vibrational modes that arise from atomic motions in the conjugated portion of nitrophenylriboamidrazone. The vibrational modes related to motion of the hydroxyl groups, for example, are not expected in the spectra. Except for the Raman bands at 1069 and 1676 cm^{-1}, the bands in Figure 3a can be assigned to the nitrophenylhydrazine fragment of nitrophenylriboamidrazone since their counterparts were

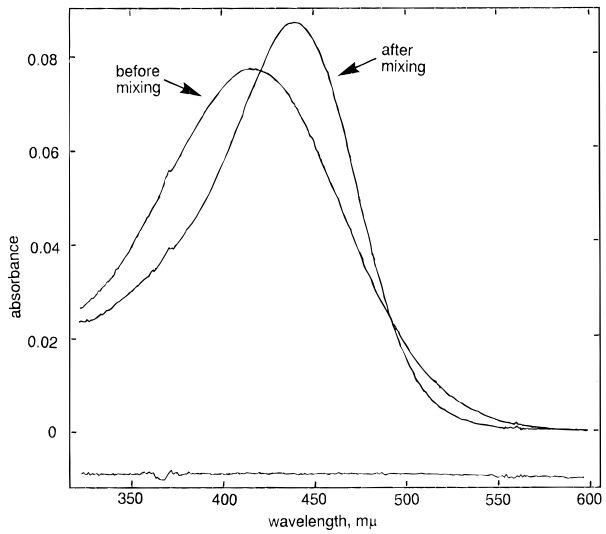

FIGURE 2: Absorption spectrum of nitrophenylriboamidrazone free and bound to IU-nucleoside hydrolase. The absorption spectrum of free nitrophenylriboamidrazone is in 20 mM Hepes buffer, pH 7.3. Samples of the enzyme−inhibitor complex used for Raman measurements showed the same spectral properties.

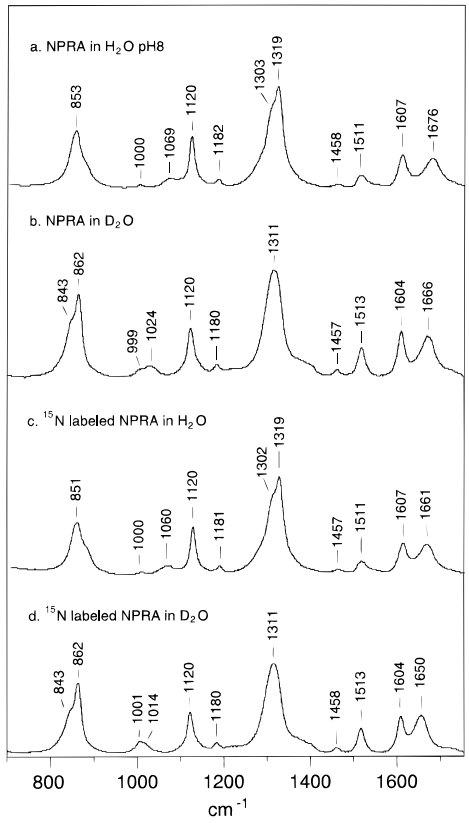

FIGURE 3: Raman spectra of a nitrophenylriboamidrazone solution (a) and its deuterated (b), $^{15}N_2$-labeled (c), and $^{15}N_2$- and deuterium-labeled (d) derivatives. The samples were prepared in 20 mM Hepes buffer at pH 8 with a nitrophenylriboamidrazone concentration of approximately 0.3 mM. The temperature of the sample was kept at 4 °C during Raman measurements; 20 mW of the 457.8 nm laser line from an argon ion laser was used for the Raman excitation. The resolution of the spectra is 8 cm^{-1}, and the Raman band positions are accurate to ±3 cm^{-1}.

readily identified in the Raman spectrum of that molecule (data not shown).

The NO_2 symmetric stretch frequency in the 1300−1350 cm^{-1} range is expected to show strong Raman intensity because the NO_2 group is conjugated in the chromophore (Daimay et al., 1991). The prominent band at 1319 cm^{-1} and the 1303 cm^{-1} band on its shoulder are assigned to the NO_2 symmetric stretch mode. The doublet nature of this mode indicates that there are two NO_2 tautomers with slightly different N−O bond strengths, perhaps due to different degrees of conjugation with the phenyl ring. The strong band at 853 cm^{-1} in Figure 3a is assigned to the NO_2 in-plane bending (sissors) mode (Daimay et al., 1991).

The broad, weak band at 1069 cm^{-1} in Figure 3a is assigned to the N1−N2 stretch mode on the basis of its 9 cm^{-1} shift to 1060 cm^{-1} upon ^{15}N labeling of N2 (Figure 1c). In the deuterated inhibitor, the N1−N2 stretch mode appears at 1024 cm^{-1} (Figure 3b) and shifts down by 10 cm^{-1} to 1014 cm^{-1} upon ^{15}N labeling (Figure 3d). The 45 cm^{-1} shift of this band upon deuteration of nitrophenylriboamidrazone (Figure 3b) indicates that the N1−N2 stretching motion is coupled with the bending motion N1−H or N2−H (Chart 2). The coupling is disturbed upon deuteration of nitrophenylriboamidrazone, resulting in a frequency shift of this mode.

The 1676 cm^{-1} band in Figure 3a can be assigned to the C1′═N2 stretch mode on the basis of its 15 cm^{-1} shift upon ^{15}N labeling of the N2 nitrogen (Figure 3c). This band is also sensitive to the deuteration of nitrophenylriboamidrazone, which causes a 10 cm^{-1} shift to 1666 cm^{-1} (Figure 3b). The shift upon deuteration for a C═N stretch mode has been observed in several Schiff base compounds where nitrogen is protonated but is not observed in unprotonated Schiff base compounds (Benecky et al., 1985; Callender & Honig, 1977; Goldberg et al., 1993; Mathies et al., 1976). Furthermore, the frequency of an unprotonated C═N stretch mode is usually lower than 1640 cm^{-1}, while the frequency of a protonated C═N(H) stretch mode is normally higher than 1650 cm^{-1} (Daimay et al., 1991). All of these comparisons with previous studies suggest that the band at 1676 cm^{-1} (Figure 3a) can be assigned to the C1′═N2(H) stretch mode from tautomer b (Chart 2b). Assignment of this band to the (H)N1═C1 stretch mode from tautomer c (Chart 2c) can be ruled out because the ab initio calculations indicate that this mode does not exhibit a large shift upon ^{15}N labeling at N2. This assignment does not rule out the existence of tautomer c in solution, since the Raman intensity of the unprotonated C═N stretch mode is smaller than the corresponding protonated C═N(H) stretch mode (Callender & Honig, 1977; Goldbert et al., 1993; Smith et al., 1986). The unprotonated C1′═N2 stretch mode of tautomer c may also shift significantly upon the deuteration of nitrophenylriboamidrazone, as suggested by normal mode calculations using ab initio quantum mechanics methods (see below). Therefore a small portion of the low-frequency side of the 1676 cm^{-1} band may be due to the C1′═N2 stretch of tautomer c.

The remaining Raman bands in Figure 3a do not shift significantly upon isotopic labeling (Figure 3b−d) or upon nitrophenylriboamidrazone binding to enzyme (Figure 4), and their assignments will not be discussed further.

Resonance Raman Spectra for Enzyme-Bound Inhibitor. The resonance Raman spectrum of nitrophenylriboamidrazone bound to nucleoside hydrolase gives the NO_2 symmetric stretch mode as a single band at 1294 cm^{-1}, indicating that the majority of the bound inhibitor exists as a single tautomer. This mode shifts from 1303 to 1319 cm^{-1} in solution to 1294 cm^{-1} on the enzyme (Figure 3a), indicating weakened N−O

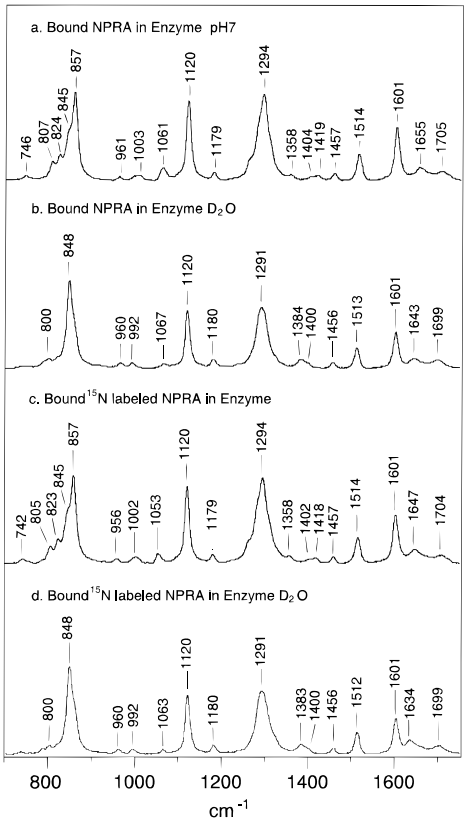

FIGURE 4: Raman spectra of nitrophenylriboamidrazone bound to nucleoside hydrolase (a) and its D_2O (b), $^{15}N_2$ (c), and $^{15}N_2 + D_2O$ (d) derivatives. A small contribution from enzyme in the original spectra has been subtracted. The sample was in 20 phosphate buffer at pH 7.2. The concentration of the enzyme was 0.3 mM, and the concentration of the inhibitor was approximately 0.2 mM as judged by the absorbance at 445 nm. Under these conditions, >99% of the inhibitor is enzyme-bound, based on the equilibrium dissociation constant of 2 nM (Boutellier et al., 1994). The temperature of the sample was kept at 4 °C during Raman measurements; 20 mW of the 457.8 nm laser line from an argon ion laser was used for the Raman excitation. The resolution of the spectra is 8 cm^{-1}, and the Raman band positions are accurate to ± 3 cm^{-1}.

bonds for the enzyme-bound ligand. The reduced N−O bond strength is correlated with an extended conjugation of nitrophenylriboamidrazone on the enzyme, also indicated by the red shift of bound inhibitor (Figure 2).

The band at 1061 cm^{-1} in Figure 4a can be assigned to the N1−N2 stretch mode on the basis of its 8 cm^{-1} shift to 1053 cm^{-1} upon ^{15}N labeling of the N2 nitrogen (Figure 4c). The frequency and the ^{15}N shift of the N1−N2 stretch mode are similar to those in solution. However, its coupling with the N−H bend motion becomes different when the inhibitor binds to the enzyme. In solution, the N1−N2 stretch mode shifts down 45 cm^{-1} to 1024 cm^{-1} upon deuterium labeling of nitrophenylriboamidrazone (Figure 3b) but still contains the N1−N2 stretch character as shown by its 10 cm^{-1} shift upon labeling with ^{15}N (Figure 3d). In contrast, the N1−N2 stretch mode of nitrophenylriboamidrazone is not observed in the enzyme upon deuteration since no Raman band in the appropriate spectral region has a comparable 10 cm^{-1} shift upon ^{15}N labeling of N2 (Figure 4b,d). The weak band at 1067 cm^{-1} in the deuterated nitrophenylriboamidrazone spectrum (Figure 4b) which is shifted 4 cm^{-1} upon ^{15}N labeling of N2 (Figure 4d) cannot be due to the vibrational mode at 1024 cm^{-1} (Figure 3b), since its frequency is higher and its ^{15}N shift is smaller. The difference between the N1−N2 stretch modes of nitrophenylriboamidrazone in solution and on the enzyme may be caused by the rotation around C1′═N2 and/or N1−N2 bonds previously proposed in order to place the *p*-nitrophenyl group in a position similar to the hypoxanthine leaving group for the transition state (Boutellier et al., 1994).

The C1′═N2(H) stretch mode found at 1676 cm^{-1} for the inhibitor in solution (Figure 3a) could be assigned to either one of two bands, at 1705 and 1655 cm^{-1} when the inhibitor is bound to the enzyme (Figure 4a). The band at 1705 cm^{-1} shifts to 1699 cm^{-1} upon deuteration of nitrophenylriboamidrazone (Figure 4b), but shows little shift upon ^{15}N labeling of N2 (Figure 4c), and therefore is not the C1′═N2 stretch mode. The band at 1655 cm^{-1} in Figure 4a can be assigned to the C1′═N2 stretch mode on the basis of its 8 cm^{-1} shift to 1647 cm^{-1} upon ^{15}N labeling of N2 (Figure 4c). The 8 cm^{-1} ^{15}N-induced shift of the C1′═N2 stretch mode on the enzyme compared with a 15 cm^{-1} shift in solution (Figure 3a,c) indicates that this mode becomes more delocalized. Another change of the C1′═N2 stretch mode when nitrophenylriboamidrazone is bound to the enzyme is an increased response upon deuteration, from a 10 cm^{-1} shift in solution (Figure 3a,b) to 12 cm^{-1} on the enzyme (Figure 4a,b). Previous studies have shown that weaker hydrogen bonding to the C═N−H hydrogen induces a downward frequency shift in the C═N(H) stretch mode, but at the same time, its frequency shift upon deuteration becomes smaller (Baasov et al., 1987; Deng & Callender, 1987; Gilson et al., 1988). Since the frequency of the C1′═N2(H) stretch mode of bound nitrophenylriboamidrazone becomes lower than in solution while its deuterium shift becomes larger, the observed results cannot be accounted by a simple change of the C1′═N2(H) hydrogen-bonding strength upon interaction with the enzyme. One explanation for the observed changes of the C1′═N2 stretch frequency and its deuterium shift could be an interaction between the NO_2 group and a positively charged protein residue. In addition, the direct interactions of a protein anion with the cationic center at C1′ could perturb the solution pattern of C1′. The C1′═N2(H) stretch mode could also differ from that of a normal Schiff base due to geometric distortion induced by the relative geometries of binding the iminoribitol and *p*-nitrophenyl groups.

Ab Initio Modeling of Nitrophenylriboamidrazone. To investigate the effects of ionic interactions, vibrational normal mode analyses by ab initio quantum mechanical methods were carried out on model compounds of the tautomers, in which the hydroxyl and methoxy groups on the iminoribitol ring were replaced by hydrogens. Calculations on the model compounds were also conducted with a cation (Na^+ ion was used in the model) complexed to the oxygens of the NO_2 group or an anion (Cl^- ion) complexed to the hydrogens on N4′ and N2.

The geometry of each tautomer of the model compound was optimized at the HF/3-21G level using Gaussian 92 (Frisch et al., 1992) prior to bond vibrational frequency analysis. The in vacuo electronic energies of tautomers a and b are 7.2 and 18.8 kcal/mol higher, respectively, than that of tautomer c (Chart 2). Subsequent frequency calculations suggest that the zero point vibrational energies differ by less than 0.5 kcal/mol among these tautomers. Thus, tautomer c should be the most likely species and tautomer b should be the least likely species for nitrophenylriboamidrazone in the gas phase. When Na^+ is bound to the NO_2 and

Table 1: Resonance Raman Bands for the C═N and C═C Stretch Modes of Nitrophenylriboamidrazone (NPRA)[a]

	mode	native	D	^{15}N	^{15}N,D
experimental					
NPRA in solution	C1′═N2(H)	1676	1666 (−10)	1661 (−15)	1650 (−11)
NPRA in enzyme	ring	1707	1699 (−6)	1704 (−1)	1699 (−5)
	C1′═N2(H)	1655	1643 (−12)	1647 (−8)	1634 (−13)
calculated					
tautomer a	C1′═N4′	1687	1679 (−7)	1685 (−1)	1678 (−7)
tautomer a + Na	C1′═N4′	1703	1697 (−6)	1703 (−1)	1696 (−6)
tautomer b	C1′═N2(H)	1667	1646 (−22)	1655 (−12)	1634 (−22)
C═N cis	ring	1582	1581	1581	1580
tautomer b	ring	1662	1656 (−7)	1658 (−4)	1654 (−5)
C═N cis + Na	C1′═N2(H)	1635	1625 (−10)	1630 (−5)	1620 (−10)
tautomer b	C1′═N2(H)	1670	1653 (−18)	1656 (−14)	1639 (−17)
C═N trans	ring	1582	1581	1581	1580
tautomer b	ring	1658	1653 (−5)	1654 (−4)	1652 (−3)
C═N trans + Na	C1′═N2(H)	1634	1618 (−17)	1627 (−8)	1611 (−16)
tautomer c	C1′═N2	1656	1642 (−14)	1643 (−13)	1627 (−16)
tautomer c + Na	C1′═N2	1644	1634 (−11)	1633 (−12)	1622 (−11)

[a] The observed modes for NPRA in solution and bound to IU-nucleoside hydrolase are compared to those determined from ab initio calculations at the HF/3-21g level. The effects of deuterium and ^{15}N substitution are indicated. Ab initio stretching frequencies are given for the three tautomers of Chart 1 with or without an associated Na^+. Two configurations of tautomer b, one with the C1′═N2 cis configuration and one with the C1′═N2 trans configuration, are studied (Chart 2b). The ring mode is the in-phase combination of the C2═C3/C5═C6 stretches. The frequencies are in cm^{-1}, and the numbers in parentheses are the frequency shift relative to that of the unlabeled molecule, except in the case of the ^{15}N,D derivative which is the frequency shift from the ^{15}N-labeled molecule.

the geometries of the complexes are fully reoptimized, the relative electronic energies of tautomers a and b are 14.2 kcal/mol higher and −0.6 kcal/mol lower, respectively, than that of tautomer c−Na^+. Tautomer b with C1′═N2 trans configuration (N4′ trans with respect to N1 as the result of a 180° rotation around C1′═N2 bond) also shows a large change in relative stability upon introduction of a Na^+ ion. The electronic energy of the C1′═N2 trans tautomer b is 23.8 kcal/mol higher than that of tautomer c when compared as unliganded molecules, but only 3.6 kcal/mol higher as the Na^+ complex.

The optimized distance between Na^+ ion and the oxygens of the NO_2 group in the model compounds varies from 2.14 to 2.20 Å, among the tautomer complexes. Thus, the strength of the NO_2−cationic group interaction is intrinsically different for the tautomers. Tautomer b forms the strongest interaction with a positively charged group, causing the energy of this inhibitor−Na^+ complex to be reduced the most when this interaction occurs. The NO_2 group of tautomer a forms a relatively weak interaction; therefore, the energy of this inhibitor−Na^+ complex does not reduce as much. Thus, the energy of the tautomer a system becomes the highest when a positively charged group interacts with the NO_2 group of nitrophenylriboamidrazone. The strength of the interaction between the NO_2 group and the external positive charge is primarily determined by the tautomeric form of the inhibitor and is less affected by the conformation of the inhibitor.

The interaction between the NO_2 group of nitrophenylriboamidrazone with H_2O or with a positive charge on the enzyme should be somewhere in between the extreme cases modeled above. Thus, a significant proportion of the inhibitor is expected to exist in tautomeric forms b and c in solution as indicated by the resonance Raman results. Tautomer a and its Na^+ complex is energetically unfavorable under all conditions, consistent with the titration and spectral studies of Figures 1 and 2.

Calculated Isotopic Stretch Frequencies for Model Nitrophenylriboamidrazones. Table 1 shows the calculated C═N stretch frequencies and their isotopic shifts for tautomer a, both configurations of tautomer b, and tautomer c, using the model compound, in the absence or presence of a Na^+ ion, calculated at the ab initio HF/3-21G level.[2] All calculated frequencies are multiplied by a factor of 0.9 for easier comparison with experimental values. Previous studies have shown that normal mode calculations using in vacuo ab initio quantum mechanics methods generally overestimate the vibrational frequencies by 10%−20%, depending on the vibrational mode or the specific method used (Pulay et al., 1983). Although these calculations are not accurate enough to reproduce the vibrational spectrum of a molecule, errors are systematic and the changes of the frequencies and the isotopic shifts of a vibrational mode induced by structural or environmental changes can often be predicted quite satisfactorily (Deng et al., 1992, 1994). This approach will be adopted here to determine the structural and environmental changes of nitrophenylriboamidrazone upon binding to nucleoside hydrolase.

Ab initio calculations predict that the highest frequency mode of the isolated tautomer a in the spectral range up to 1800 cm^{-1} is a C═N stretch mode which has a shift of 7 cm^{-1} upon deuteration of the molecule and a 1 cm^{-1} shift upon ^{15}N labeling of N2. Examination of the atomic displacements reveals that this mode is the C1′═N4′ stretch mode, with little motion of the N2 nitrogen. Another mode which is related to the in-phase combination of the C2═C3/C5═C6 stretch motions of the phenyl ring is about 100 cm^{-1}

[2] The 3-21g basis set used in these calculations is superior to more complete basis sets such as 4-31G* or 6-31G** for frequency calculations involving coupled C═C and C═N or C═C and C═O bonds (Deng et al., 1992, 1994). The basis sets with polarization functions (denoted by the * sign) overestimate the frequency of the C═N or C═O stretch mode more than that of the C═C stretch mode so that the vibrational coupling between the C═C stretch and the C═N or C═O stretch is usually underestimated.

lower than the C1′═N4′ stretch mode, and it is not sensitive to deuterium or ^{15}N labeling.

When tautomer a is complexed with a Na^+ ion, the calculated C1′═N4′ stretch mode frequency shifts up by 17 cm^{-1} and is still insensitive to the ^{15}N labeling at N2. The calculated frequency of the ring mode does not change, indicating that the interaction between the NO_2 group and the cation is not strong enough to change the electron distribution of the C2═C3/C5═C6 bonds of the phenyl ring. The calculated isotopic shifts of this tautomer are inconsistent with the Raman spectra of nitrophenylriboamidrazone in solution or enzyme-bound; thus the presence of this tautomer can be ruled out.

In the Raman spectral region of interest, the highest frequency mode for isolated tautomers b or c is the C1′═N2 stretch mode. The frequency of the unprotonated C1′═N2 stretch in tautomer c is 10 cm^{-1} lower than the C1′═N2(H) stretch of tautomer b, similar to the differences upon protonation of a normal Schiff base compound (Benecky et al., 1985; Goldberg et al., 1993). The C1′═N2 stretch mode for tautomer c is predicted to have a frequency shift of 14 cm^{-1} upon deuteration of the model compound, quite similar to the calculated deuterium shift of the C1′═N2(H) stretch mode of tautomer b (Table 1). The exact values of the isotopic shifts are sensitive to the conformation of the tautomer. For example, the deuterium and ^{15}N shifts of the C1′═N2(H) mode of tautomer b with the C1′═N2 cis configuration (shown in Chart 2b) are 22 and 12 cm^{-1}, respectively. When the C1′═N2 configuration of the tautomer b is changed to trans, the isotopic shifts of the C1′═N2(H) stretch mode become 18 and 14 cm^{-1} upon deuterium and ^{15}N labeling, respectively. The calculated frequencies of the ring mode in isolated tautomer b and tautomer c are within 5 cm^{-1} of each other and shift little (<2 cm^{-1}) upon deuterium or ^{15}N labeling, suggesting that this mode is localized.

When the model compound is complexed to Na^+, the normal modes of tautomer c in the C═C and C═N stretch region change differently compared to those of tautomer b. The C1′═N2 stretch frequency of tautomer c becomes ∼12 cm^{-1} lower and its deuterium shift decreases by 3 cm^{-1} upon complexation of a Na^+ ion, but its shift upon ^{15}N labeling at N2 is little changed. The frequency of the ring mode, which results from the in-phase C2═C3/C5═C6 stretch combination, is predicted to shift up by 11 cm^{-1} due to the increased double bond character in these bonds when complexed with Na^+. Since this mode is localized to the ring, it shifts little upon deuterium or ^{15}N labeling. When the Na^+ ion is forced toward the NO_2 group of tautomer c to reduce the distance between the Na^+ and the oxygens of NO_2 to 2.0 Å (compared with 2.14 Å in tautomer b−Na^+ complex), the calculated C1′═N2 stretch mode is still 45 cm^{-1} higher than the in-phase C2═C3/C5═C6 stretch mode and shows little change in its frequency shift upon ^{15}N labeling at N2. This result indicates that no coupling exists between the C1′═N2 stretch and the in-phase C2═C3/C5═C6 stretch motions.

The tautomer b system responds differently to the nitro−cation interaction, with this spectral region being widely disrupted when the Na^+ binds. Ab initio calculations predict that the double bond character of the C2═C3 and C5═C6 bonds is fully developed, and the double bond character of C1′═N2 is significantly reduced, while that of C1′−N4′ is greatly increased as depicted in Chart 2. The stretch motions of these three double bonds are coupled strongly to form two new vibrational modes. In the C1′═N2 cis configuration, the mode with the highest frequency in this region shows small shifts, 7 and 4 cm^{-1} upon deuterium and ^{15}N labeling, respectively. Another mode, 27 cm^{-1} below the highest frequency mode, shows shifts of 10 and 5 cm^{-1}, upon deuteration and ^{15}N labeling, respectively. The degree of coupling between the in-phase C2═C3/C5═C6 stretch and the C1′═N2 stretch is most sensitive to the strength of the interaction between the NO_2 group and the external positive charge. The conformation of the tautomer also influences the coupling between the two types of stretch motions. For example, in tautomer b with the C1′═N2 trans configuration, deuterium and ^{15}N shift the lower frequency mode of the coupled pair by 17 and 8 cm^{-1}, respectively, indicating a larger contribution from the C1′═N2 stretch compared with the cis configuration. Conformational changes of tautomer b, such as the twist around C1′═N2 and/or N1−N2 bonds, change the coupling between the C1′═N2(H) stretch and the in-phase C2═C3/C5═C6 stretch, but do not eliminate the coupling.

Assignment of Resonance Raman Spectral Features for Enzyme-Bound Nitrophenylriboamidrazone. The band at 1705 cm^{-1} in Figure 4a is assigned to the in-phase combination of the C2═C3/C5═C6 stretches of tautomer b coupled with the C1′═N2(H) stretch motion to give a 6 cm^{-1} shift upon deuteration of nitrophenylriboamidrazone (Figure 4b). The unusually high frequency of this mode reflects the strengths of the C2═C3 and C5═C6 bonds when nitrophenylriboamidrazone binds to enzyme. The increased bond strengths of these two bonds require a strong interaction between the NO_2 group of the inhibitor and a positively charged enzyme residue(s). This interaction also increases the conjugation and results in a weakened C1′═N2 bond and a red-shifted C1′═N2(H) stretch mode. Thus, the band at 1655 cm^{-1} in Figure 4a can be assigned to the C1′═N2(H) stretch mode of tautomer b. Since it is coupled with the in-phase combination of the C2═C3/C5═C6 stretches, its shift upon ^{15}N labeling of N2 becomes smaller than that in aqueous solution (Figure 4c).

The interaction between the NO_2 group of nitrophenylriboamidrazone and a positively charged enzyme residue cannot explain all spectral changes of bound inhibitor. Ab initio calculations predict a reduced (in tautomer b with the C1′═N2 cis configuration) or unchanged (in tautomer b with the C1′═N2 trans configuration) shift in the C1′═N2(H) mode upon deuteration of nitrophenylriboamidrazone in the Na^+ complex compared with that of the isolated tautomer (Table 1). The observed deuterium shift is a relative *increase* in the C1′═N2(H) stretch mode for bound nitrophenylriboamidrazone. This discrepancy can be explained by anionic assistance to the hydrogen bonding on N2. Ab initio calculations for tautomer b, C1′═N2 trans, complexed with an anion[3] which interacts with hydrogens on the N4′ and N2 nitrogens, demonstrates that the frequency of the C1′═N2(H) stretch mode in this complex increases by 18 cm^{-1} and thus, its deuterium shift increases by 8 cm^{-1}. Similar results have been observed with a normal Schiff base (Baasov et al., 1987; Deng & Callender, 1987; Gilson et al.,

[3] The anionic group on the enzyme is likely to be a carboxylate. To simplify the ab initio Gaussian 92 calculations, the model calculations used a chloride anion to generate the negative charge.

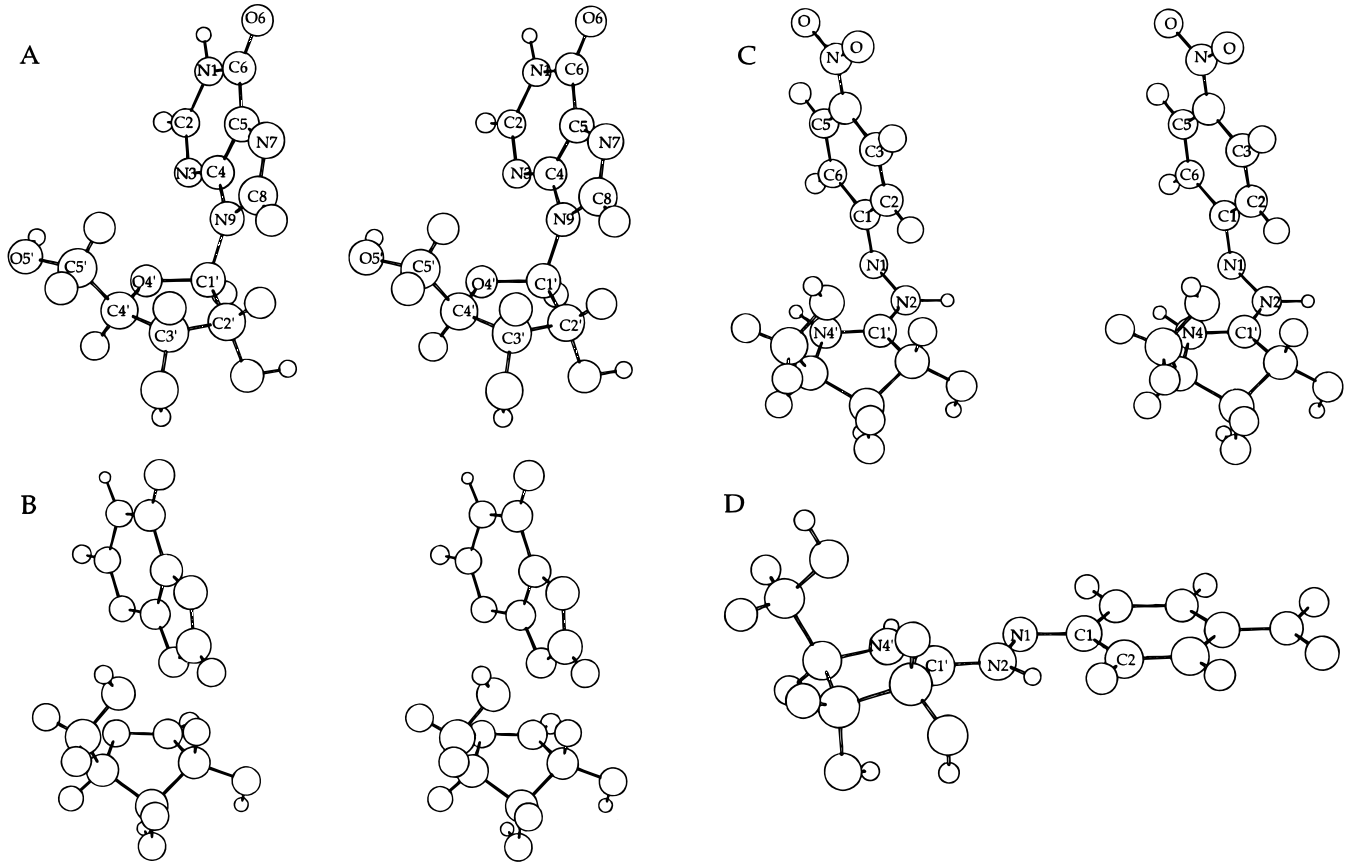

FIGURE 5: Stereoviews of the geometric structures of inosine (A), the transition state (B), nitrophenylriboamidrazone near an energetic minimum to mimic the geometry of the transition state structure (C), and a monoview of the extended structure for nitrophenylriboamidrazone expected in solution (D). The geometries of (A), (B), and (C) are the same as used in the electrostatic potential surfaces shown in Figure 6.

1988). The red-shifted frequency and the increased shift upon deuteration for the C1′═N2(H) stretch mode of bound inhibitor can be explained by a cationic interaction with NO_2 and an anionic interaction with the H−N4′−C1′═N2-H region of nitrophenylriboamidrazone.

Ab initio calculations suggest that the alternative assignment of the 1705 and 1655 cm^{-1} bands to tautomer c is unlikely because no chemically reasonable interaction can reduce the bond strength of C1′═N2 in tautomer c to cause the downshift of its stretching frequency below that of the C2═C3/C5═C6 in-phase stretch mode.

DISCUSSION

Tautomeric Forms of Free and Bound Nitrophenylriboamidrazone. In aqueous solution at pH 8, nitrophenylriboamidrazone exists as a mixture dominated by two tautomeric forms, with one proton at N4′ and the other proton shared between N1 or N2 (tautomers b and c, Chart 2). On binding to the enzyme, the tautomer with protonated N4′ and N2 predominates. The resonance Raman data cannot resolve the cis/trans C1′═N2 bond configuration, but ab initio calculations show that tautomer b, C1′═N2 cis, has a small energetic advantage. This configuration is also predicted from the transition-state structure of the enzyme which requires leaving group departure from the β-anomeric face of the ribosyl (Horenstein & Schramm, 1993a). In this tautomer, the only rotational degree of freedom is about the N_1-N_2 bond.

The conformation of nitrophenylriboamidrazone on the enzyme is influenced by the strong interaction between the NO_2 group and a protein residue which enhances the conjugation. In solution, this interaction would act to flatten the molecule and would favor a geometry in which the two rings exist in the same plane. If nitrophenylriboamidrazone is binding as an isostere of the transition state (Boutellier et al., 1994), the nitrophenyl ring should be positioned above and almost perpendicular to the iminoribitol ring (Figure 5). Large changes have been observed in the N1−N2 stretch mode region of the nitrophenylriboamidrazone Raman spectrum when nitrophenylriboamidrazone binds to enzyme. These have the potential to provide dihedral bond angle information for the C1′═N2 and N2−N1 bonds. However, interpretation of these data will require additional computational and model compound studies, beyond the scope of the present work.

The addition of the NO_2 group to the phenyl ring to give nitrophenylriboamidrazone provides −2.8 kcal/mol of energy toward inhibitor binding. Part of the increased binding energy appears to be contributed from the favorable interaction between the NO_2 group and a positively charged enzyme residue(s). Ab initio calculations indicate that a symmetrically placed external charge with respect to the NO_2 group will affect its symmetric stretch frequency by no more than a couple of cm^{-1} even for interaction energies of more than 10 kcal/mol. The large shift observed when nitrophenylriboamidrazone binds to nucleoside hydrolase indicates that the positively charged protein residue which

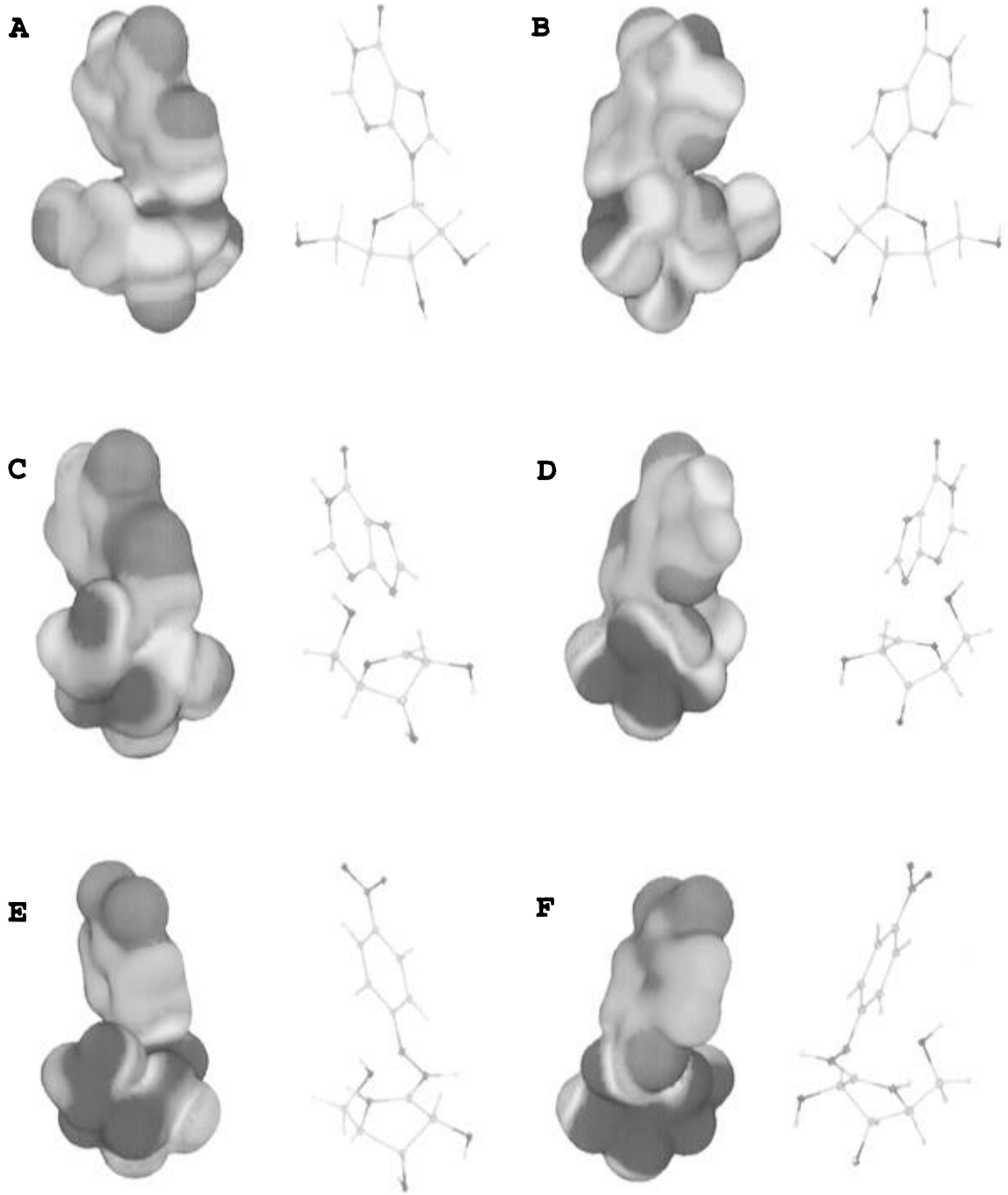

FIGURE 6: Electrostatic potential surfaces of inosine (A and B), inosine at the transition state of nucleoside hydrolase (C and D), and nitrophenylriboamidrazone (E and F). The electrostatic potential surfaces of inosine and the N-7 protonated transition state for inosine were previously determined (Horenstein & Schramm, 1993a,b). In the surfaces shown here, the geomery of inosine and the transition state were aligned to permit the best match between substrate, transition state, and inhibitor by fixing the dihedral of inosine and the transition state to C2′−C1′−N9−C8 = 0°. Each left-right panel pair shows 180° vertical rotational views of the same atomic structure. The color code for the stick figures is oxygen = red, nitrogen = blue, carbon = green, and hydrogen = white. The molecular electrostatic potential surfaces show partial negative charge (electron excess) as blue and partial positive charge (electron deficiency) as red. Yellow represents average electrostatic potential near the van der Waals surface from the entire molecular surface. The electron density is depicted at 0.002 electron per $Bohr^3$, which approximates the van der Waals surface. The hydroxyl nucleophile and the enzyme-donated proton at N7 have been removed to illustrate the electronic properties of the transition state without enzymatic contributions. Both the attacking oxygen nucleophile and the proton donated to N7 are provided by the enzyme during catalysis or the binding of inhibitors. The molecular electrostatic potential surface of nitrophenylriboamidrazone (E and F) was calculated for the conformation which most closely approximately that of the transition state (Boutellier et al., 1994).

interacts with the nitro moiety is placed asymmetrically and interacts much more strongly with one nitro oxygen than the other; asymmetrically placed charges yield much larger frequency shifts in the calculations. As is seen below, this is consistent with the proposed transition-state structure which places a substantial protein−substrate charge interaction to one side of the phenyl ring.

A protonated histidine has been implicated from pH studies (Parkin & Schramm, 1995) and the recent X-ray structure.[1] Since the interaction between the NO_2 group of nitrophenylriboamidrazone and enzyme is expected to polarize the inhibitor to increase the positive charge on the N4′(H)−

C1′═N2(H), increased binding energy may also be contributed by the strengthened interaction between the N4′(H)−C1′═N2(H) region and its negatively charged protein environment.[3]

Molecular Electrostatic Potential Surfaces of Substrate and Transition State. Molecular electrostatic potential surfaces of inosine, the transition state for inosine hydrolysis by nucleoside hydrolase, and nitrophenylriboamidrazone are compared in Figure 6. Hydrolysis of inosine by nucleoside hydrolase is a concerted process which gives kinetic isotope effects suggesting a transition state with (1) a change in ribose ring pucker from 3′-endo to 3′-exo, (2) distortion of the sp^3 geometry of the C4′ and C5′ atoms, which is proposed to position the 5′-hydroxyl group above the plane of the ribose ring, (3) rehybridization of C1′ from sp^3 to near sp^2 geometry, (4) protonation of N7 by an enzymatic group, (5) bond loss in the C1′−N9 ribosidic bond to a Pauling bond order of 0.22 (a bond length of 1.97 Å), (6) weak participation of an enzyme-bound and activated water nucleophile to form a bond order of approximately 0.01, and (7) accumulation of substantial positive charge in the ribosyl group (Horenstein et al., 1991; Horenstein & Schramm, 1993a). Defining features of the transition state are the near oxocarbenium ion nature of the ribosyl group with the subsequent change to 3′-exo geometry and N7 protonation. Electron deficiency in the ribose results from a substantial loss of the C1′−N9 ribosidic bond without yet being compensated by the lagging attack of the water oxygen. Protonation of N7 prior to complete C1′−N9 bond loss also imparts an electron deficiency in the leaving group hypoxanthine. The electrostatic features developed at the van der Waals surface of the transition state can be seen by comparing the molecular electrostatic potential surfaces of inosine (Figure 6A,B) with those of the transition state (Figure 6C,D). The attacking water nucleophile and enzyme-donated protons have been omitted from these structures for ease of comparison. At the transition state, the enzyme-bound water is 3.0 Å from C1′ of the ribose. The oxygen atom water, C1′, and N9 form a linear or near-linear reaction coordinate. The partial positive charge of the oxocarbenium is not localized at a single atomic site of the transition state but is distributed across the family of atoms which surround C1′ of the ribosyl, which is the center of the asymmetric reaction coordinate. Departure of the C1′−N9 bonding electrons into the conjugated hypoxanthine ring changes the electrostatic potential of several atoms of the purine ring to an increased negative electrostatic potential at the transition state (Figure 6).

Molecular Electrostatic Potential Features of the Transition-State Inhibitor. Transition state inhibitors interact with their cognate enzymes with high specificity and large binding energies by mimicking the physicochemical features of the enzyme-stabilized transition state. Transition-state features cause the protein to fold into a stable complex which resembles that of the transition state for catalysis. A difference between substrate-induced achievement of the enzymatic transition-state complex and transition-state inhibitor-induced folding of the enzyme complex is that the substrate is remarkably efficient at inducing the changes required to achieve the catalytically competent transition state. The catalytic turnover number for IU-nucleoside hydrolase is 32 s^{-1}, requiring millisecond reorganizations. Since it is impossible to reproduce the nonequilibrium bond lengths and charges of an actual transition state, nitrophenylriboamidrazone is only an approximate mimic. The slow-onset inhibition commonly seen with nitrophenylriboamidrazone and other transition state-inhibitors is likely a reflection of the inexact nature of these analogues (Boutellier et al., 1994; Merkler et al., 1990; Morrison & Walsh, 1988). The tight-binding component represents the inability of the complex to achieve bond cleavage and thus escape the strong and cumulative binding energy of the transition-state complex.

For IU-nucleoside hydrolase, features of the transition state include several new hydrogen bond acceptor and donor sites on inosine, new ionic bonds to the oxocarbenium ion and to the leaving group, and the potential for hydrophobic interactions with the leaving group. Many of these features are present in the transition-state inhibitor. The electrostatic potential surface of the amidrazone is shown in Figure 6E,F. The *p*-nitrophenyl group is shown in an energetically favorable geometry similar to that of the departing hypoxanthine at the transition state for enzymatic inosine hydrolysis. The change in geometry from a roughly planar one has little influence on the conjugation and bond orders. In one ab initio calculation where the N1−N2 bond is twisted by 80°, the energy of the system increased by only 3.6 kcal/mol and the conjugation of the molecule from NO_2 through the C1′═N4′ bond was not altered.

The hydrophobic surface of the phenyl ring carries a slight negative charge and occupies a similar volume as hypoxanthine at the transition state. The NO_2−cation interaction from the enzyme is not shown. Since this is likely to be the same interaction which protonates N7 of leaving group hypoxanthine at the transition state, the transition state for inosine is also shown without the cationic interaction which leads to N7 protonation. In the inhibitor, the oxygens from the *p*-nitro group straddle the position corresponding to that of O6 from inosine at the transition state with the conjugated rings located approximately 1 Å apart in parallel planes. Protonation by the same enzymatic group would give a protonated N7 for the transition state or an ionic pair interaction with the nitro group. The positive charge of the oxycarbonium at the transition state is centered at C1′ of the ribose. The tautomer of nitrophenylriboamidrazone stabilized on the enzymatic surface also localizes the positive charge near C1′. The crystal structure of the enzyme shows a cluster of carboxylates in this region,[1] and the red-shifted frequency of C1′═N2(H) for the inhibitor bound to the enzyme is consistent with the carboxylate interaction near C1′ of bound inhibitor. The sp^2-hybridized C1′ in both the transition state and the inhibitor favors the 3′-exo conformation of the ribosyl group.

Conclusions. The transition-state mimic nitrophenylriboamidrazone is bound to IU-nucleoside hydrolase as the neutral zwitterion. The delocalized positive charge at C1′ of the iminoribitol closely matches that of the ribosyl oxocarbenium ion. The nitro group of the *p*-nitrophenyl carries a distributed negative charge, as does the hypoxanthine leaving group prior to protonation. The hydrazine group provides the features of rotational and tautomeric flexibility to permit adoption of both the geometry and charge distribution of the transition state.

REFERENCES

Baasov, T., Friedman, N., & Sheves, N. (1987) *Biochemistry 26*, 3210−3217.

Beilstein, F. K. (1932) *Beilsteins Handbuch der Organischen Chemie*, 1st ed., Vol. 15, p 468, Springer, Berlin.
Benecky, M. J., Copeland, R. A., Hays, T. R., Lobenstine, E. W., Rava, R. P., Pascal, R. A. J., & Spiro, T. G. (1985) *J. Biol. Chem. 260*, 11663−11670.
Boutellier, M., Horenstein, B. A., Semenyaka, A., Schramm, V. L. & Ganem, B. (1994) *Biochemistry 33*, 3994−4000.
Callender, R., & Honig, B. (1977) *Annu. Rev. Biophys. Bioeng. 6*, 33−35.
Callender, R., & Deng, H. (1994) *Annu. Rev. Biophys. Biomol. Struct. 23*, 215−245.
Daimay, L.-V., Colthup, N. B., Fateley, W. G., & Grasselli, J. G. (1991) *The Handbook of Infrared and Raman Characteristic Frequencies of Organic Molecules*, Academic Press, San Diego.
Degano, M., Gopaul, D. N., Scapin, G., Schramm, V. L., & Sacchettini, J. C. (1996) *Biochemistry 35*, 5971−5981.
Deng, H., & Callender, R. H. (1987) *Biochemistry 26*, 7418−7426.
Deng, H., Zheng, J., Burgner, J., & Callender, R. (1989) *Proc. Natl. Acad. Sci. U.S.A. 86*, 4484−4488.
Deng, H., Burgner, J., & Callender, R. (1992) *J. Am. Chem. Soc. 114*, 7997−8003.
Deng, H., Goldberg, J. M., Kirsch, J. F., & Callender, R. (1993a) *J. Am. Chem. Soc. 115*, 8869−8870.
Deng, H., Ray, W. J., Burgner, J. W., & Callender, R. (1993b) *Biochemistry 32*, 12984−12992.
Deng, H., Huang, L., Groesbeek, M., Lugtenburg, J., & Callender, R. H. (1994) *J. Phys. Chem. 98*, 4776−4779.
Frisch, M. J., Trucks, G. W., Hend-Gordon, M., Gill, P. M. W., Wong, M. W., Foresman, J. B., Johnson, B. G., Schlegel, H. B., Robb, M. A., Replogle, E. S., Gomperts, R., Andres, J. L., Raghavachari, K., Binkley, J. S., Gonzalez, C., Martin, R. L., Fox, D. J., DeFrees, D. J., Baker, J., Stewart, J. J. P., & Pople, J. A. (1992) *Gaussian 92 user's guide*, Gaussian Inc., Pittsburgh, PA.
Gilson, H. S. R., Honig, B. H., Croteau, A., Zarrilli, G., & Nakanishi, K. (1988) *Biophys. J. 53*, 261−269.
Goldberg, J. M., Zheng, J., Deng, H., Chen, Y. Q., Callender, R., & Kirsch, J. F. (1993) *Biochemistry 32*, 8092−8097.
Gopaul, D. N., Meyer, S. L., Degano, M., Sacchettini, J. C., & Schramm, V. L. (1996) *Biochemistry 35*, 5963−5970.
Horenstein, B. A., & Schramm, V. L. (1993a) *Biochemistry 32*, 7089−7097.
Horenstein, B. A., & Schramm, V. L. (1993b) *Biochemistry 32*, 9917−9925.
Horenstein, B. A., Parkin, D. W., Estupiñán, B., & Schramm, V. L. (1991) *Biochemistry 30*, 10788−10795.
Lamotte-Brasseur, J., Dive, G., Dehareng, D., & Ghuysen, J.-M. (1990) *J. Theor. Biol. 145*, 183.
Mathies, R., Oseroff, A. R., & Stryer, L. (1976) *Proc. Natl. Acad. Sci. U.S.A. 73*, 1−5.
Merkler, D. J., Brenowitz, M., & Schramm, V. L. (1990) *Biochemistry 29*, 8358−8364.
Miller, R. L., Sabourin, C. L. K., Krenitsky, T. A., Berens, R. L., & Marr, J. J. (1984) *J. Biol. Chem. 259*, 5073.
Morrison, J. F., & Walsh, C. T. (1988) *Adv. Enzymol. Relat. Areas Mol. Biol. 61*, 201−301.
Parkin, D. W., Horenstein, B. A., Abdulah, D. R., Estupiñán, B., & Schramm, V. L. (1991) *J. Biol. Chem. 266*, 20658−20665.
Pulay, P., Fogarasi, G., Pongor, G., Boggs, J. E., & Vargha, A. (1983) *J. Am. Chem. Soc. 105*, 7037.
Sjoberg, P., & Politzer, P. (1990) *J. Phys. Chem. 94*, 3959−5961.
Smith, S. O., Hornung, I., Steen, R. V. D., Pardoen, J. A., Braiman, M. S., Lugtenburg, J., & Mathies, R. A. (1986) *Proc. Natl. Acad. Sci. U.S.A. 83*, 967−971.
Venanzi, C. A., Plant, C., & Vananzi, T. J. (1992) *J. Med. Chem. 35*, 1643−1649.

BI9526544